Surface Structure of CdSe Nanorods Revealed by Combined X-ray Absorption Fine Structure Measurements and *Ab-initio* Calculations

Supporting information

Deborah M. Aruguete, Matthew A. Marcus, Liang-shi Li[†]*, Andrew Williamson, Sirine Fakra, Francois Gygi*[‡]*, Giulia A. Galli*[‡]*, and A. Paul Alivisatos*[*]

Department of Chemistry, University of California at Berkeley, Berkeley, CA 94720

Advanced Light Source, Lawrence Berkeley National Laboratory, Berkeley, CA 94720

Quantum Simulations Group, Lawrence Livermore National Laboratory, Livermore, CA 94550

I. Analysis

A. Use of k^2 weighting.

We used k^2 weighting as opposed to a k^3 weighting for two primary reasons. First, we did not wish to overweight the higher k data, as it had more noise. Second, we believe that the k^2 weighting was adequate for canceling out multiple-scattering effects present in the low-k data. This is because the reference phase and amplitude functions used in our fitting are from a reference that is very similar to our nanorod sample, namely bulk CdSe. In this way, we account for many of the multiple-scattering effects that are present at low k.

B. Inclusion of asymmetry in analysis

Asymmetry was included in our fits by replacing the assumed Gaussian radial distribution with a Gaussian-broadened exponential tail function, the width of the exponential part being a measure of the third cumulant.[1]

C. Angular distributions of the nanorods, and determination of $\langle \cos^2 q \rangle$

q is defined as the angle between the c-axes of the nanorods and the X-ray polarization. Angular distributions of the nanorods were determined by azimuthal integration of the 002 reflection intensity. Peaks in the intensity were fitted with Gaussian functions. The quantity reported is the numerically-integrated average of $\cos^2 q$, not the $\cos^2$ of the average q. This distinction is important because it is the former quantity which is relevant to the EXAFS.

Table S1. Angular distributions of CdSe nanorod liquid crystals

<*q*>	FWHM
20.3	50
65.7	30
66.4	30
70.3	48
110.3	33
137.4	34
132.8	30
128.7	64
157.1	29
159.1	48
204.7	30
226.4	38
222.9	28
231.9	37
248.5	30

D. Alternate fitting procedure

Spectra at all angles were fit simultaneously to minimize residual error expressed as the following summation over the filtered spectra *i* and all *k*-values *k*:

$$\sum_{i,k}\left\{ c_i(k) - \left[\left\langle \sin^2 q \right\rangle c_{fit}(r_\perp, b_\perp, s_\perp^2, \Delta E_{0\perp}, k) + \left\langle \cos^2 q \right\rangle c_{fit}(r_\parallel, b_\parallel, s_\parallel^2, \Delta E_\parallel, k) \right] \right\}^2$$

where *b* is the ratio of the coordination number of a given shell to its value in the bulk, *r* is the interatomic distance, s^2 is the mean-squared relative displacement (spread in distance distribution), ΔE_0 is a shift in the E_0 value (the energy origin, or position of the edge step). Values of *r*, *b*, s^2, and ΔE_0 are thus obtained for the parallel and perpendicular orientations of the rod *c*-axes relative to the X-ray polarization. By fitting

all spectra simultaneously, the ratio of the degrees of freedom to the parameters fit was maximized.

Tables S2 and S3 show the anisotropies and 1-σ in interatomic distances, coordination numbers (not fractional), and mean-squared relative displacements (s^2) obtained from this fitting.

Table S2. 1st shell anisotropies

	$r_\perp - r_\parallel$ (Å)	$CN_\perp - CN_\parallel$	$s^2_\perp - s^2_\parallel$ (10^{-4} Å^2)
Aligned sample	0.000(+0.001,-0.002)	0.044(+0.076,-0.080)	0.55(+1.45,-1.55)
Isotropic	0.000(+0.001, -0.001)	-0.332(+0.368,-0.4322)	-0.41(-6.41,-6.59)

Table S3. 2nd shell anisotropies

	$r_\perp - r_\parallel$ (Å)	$CN_\perp - CN_\parallel$	$s^2_\perp - s^2_\parallel$ (10^{-4} Å^2)
Aligned sample	-0.014(+0.008,-0.006)	0.044(+0.076,-0.080)	0.55(+1.45,-1.55)
Isotropic	-0.001(+0.006, -0.008)	-0.332(+0.368, -0.432)	-0.41(+6.41,-6.59)

II. Concerning usage of empirical standards

A. Hole effect.

The hole effect in bulk CdSe was checked for by comparing data taken on different bulk samples. No differences in EXAFS amplitudes were found.

B. Split first- and second-shell distances in bulk standard

We fit our EXAFS data to amplitude and phase functions derived from measurements of empirical standards. For bulk CdSe, we assume a single average distance, rather than two different distances as are actually present. The bonds along the

c-axis are 0.005 Å longer than the rest of the bonds. There are two different Se-Se distances as well; those along the *c*-axis are shorter. Here, we show that the effect of having two different distances present (for first and second shell distances) is insignificant and hence our assumption is valid.

There are two distances present for both the first shell and second shell in CdSe. The distribution of these distances can be described as the following:

$$P(r) = x\delta(r - r_1) + (1 - x)\delta(r - r_2). \quad (1)$$

For 1NN distances, $x = 0.75$, and for 2NN distances, $x = 0.5$.

With a standard cumulant expansion[2,3], the EXAFS signal can be expressed as

$$c(k) = \mathrm{Im}\left[A(k) e^{2ik\langle r\rangle - 2k^2\sigma^2 - \frac{4}{3}ik^3 C_3 + \ldots} \right]. \quad (2)$$

Hence, a distribution of bonds in the standard will affect the anharmonicity term C_3. As $C_3 = \left\langle (r - \langle r \rangle^3) \right\rangle$, using the distribution $P(r)$ given in eqn 1, we find

$$C_3 = x(1 - x)(1 - 2x)(r_1 - r_2)^3, \quad (3)$$

which, for $x = 3/4$ and a bond distance difference of 0.005 Å, is -1.17×10^{-8} Å. The contribution of the bond distance distribution to anharmonicity is much smaller than previously measured values for bulk cadmium selenide; C_3 was measured at 250 K (with 18 K data as a reference) to be $\sim 8 \times 10^{-5}$ Å^3[4]. For the 2NN distances, $x = 1/2$, which makes $C_3 = 0$. We can therefore conclude that our assumption of an averaged bond value for our CdSe standard is valid.

(1) Marcus, M. A.; Chen, H. S.; Espinosa, G. P. *Solid State Communications* **1986**, *58*, 227.

(2) Bunker, G. *Nucl. Instrum. Methods Phys. Res.* **1983**, *207*, 437.

(3) Crozier, E. D.; Rehr, J. J.; Ingalls, R. Amorphous and Liquid Systems. In *X-ray absorption: Principles, applications, techniques of EXAFS, SEXAFS, and XANES*; D.C.Koningsberger, Prins, R., Eds.; John Wiley and Sons: New York, 1988.

(4) Dalba, G.; Fornasini, P.; Grisenti, R.; Pasqualini, D.; Diop, D.; Monti, F. *Physical Review B: Condensed Matter and Materials Physics* **1998**, *58*, 4793.

Figure S1. Raw dichroism data

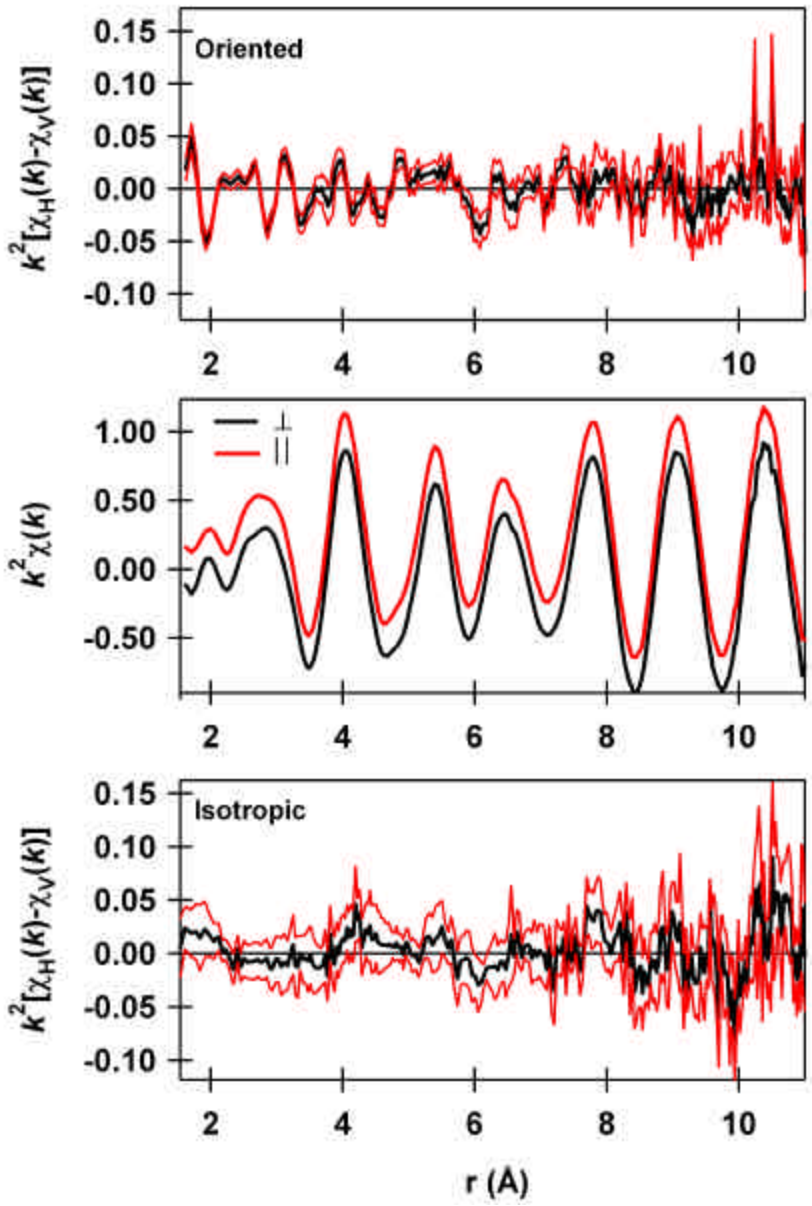

Figure S1. Due to the uniaxial symmetry of the nanorods, we can express the angular dependence of the K-edge EXAFS signal for a given atomic coordination shell as the following:

$$c(k,q) = \left[c_{\|}(k) - c_{\perp}(k) \right] \left\langle \cos^2 q \right\rangle + c_{\|}(k)$$

where $c_{\|}(k)$ and $c_{\perp}(k)$ are the EXAFS when the rod c-axes are parallel and perpendicular to the x-ray beam polarization. The difference $c_{\|}(k) - c_{\perp}(k)$ is defined as the absorption dichroism. The $\left\langle \cos^2 q \right\rangle$ values were obtained experimentally from XRD. By fitting $c(k)$ measured at fifteen different angles to this equation, we obtained the dichroism, as well as $c_{\|}(k)$ and $c_{\perp}(k)$, as shown in the top and middle plots of this figure, respectively. ($c_{\|}(k)$ is displaced slightly upwards for visibility.) A control study was also conducted on isotropic or non-aligned nanorods; the resulting lack of dichroism is evident in the bottom plot. It should be noted that the data for the isotropic were not of as good quality nor taken for as many angles as that for the liquid crystal, which is why the error bands are larger.

Figure S2. Fourier transform magnitudes for bulk CdSe, nanorods, and chemical standards of possible surface species. (Imaginary signal components also displayed for bulk and nanorod CdSe.)

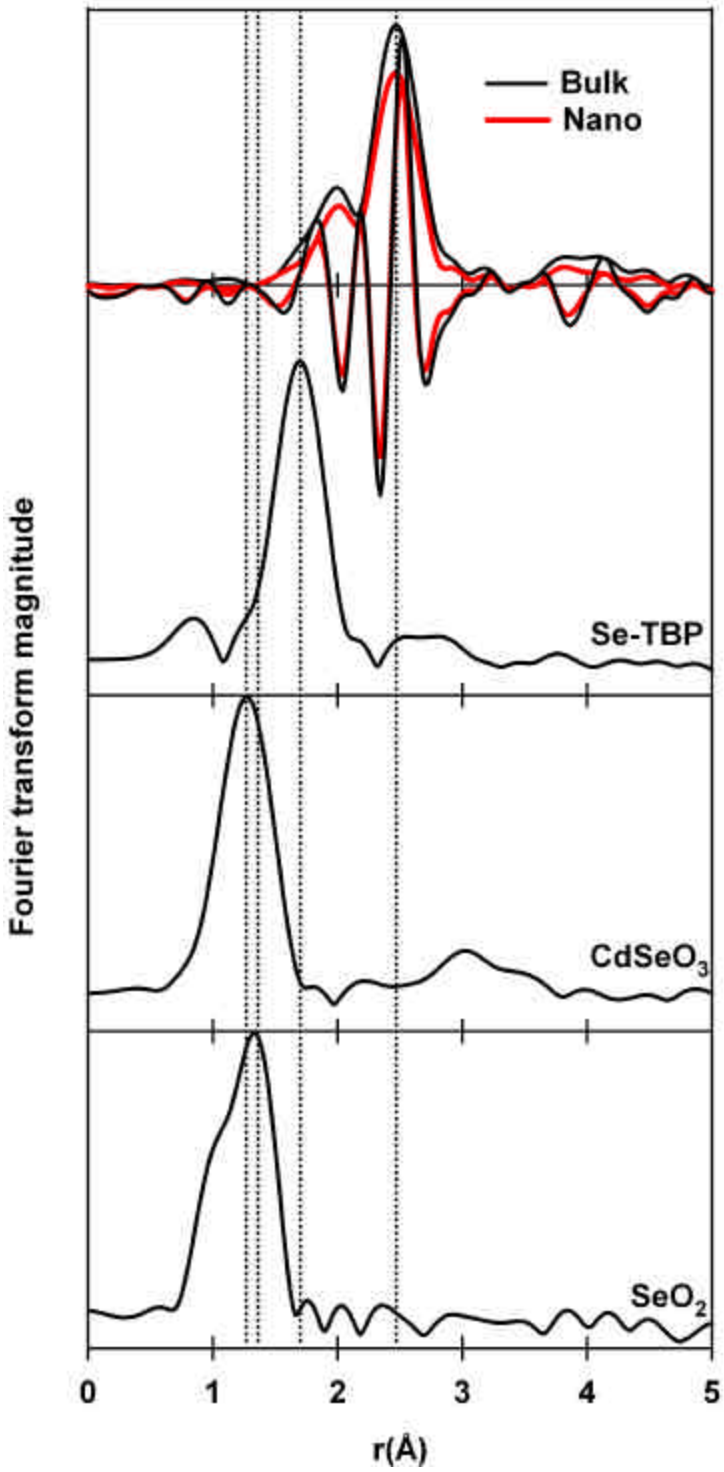

Figure S2. Experimental pair distribution functions of bulk and nanorod CdSe, as well as likely surface oxides and selenium-tributylphosphine (Se-TBP), a synthetic precursor. Imaginary components of the Fourier transformed data are displayed along with the magnitudes for bulk and nanorod CdSe.

Figure S3. Fourier transform magnitudes derived from FEFF 8.1 calculations on nanowire simulations

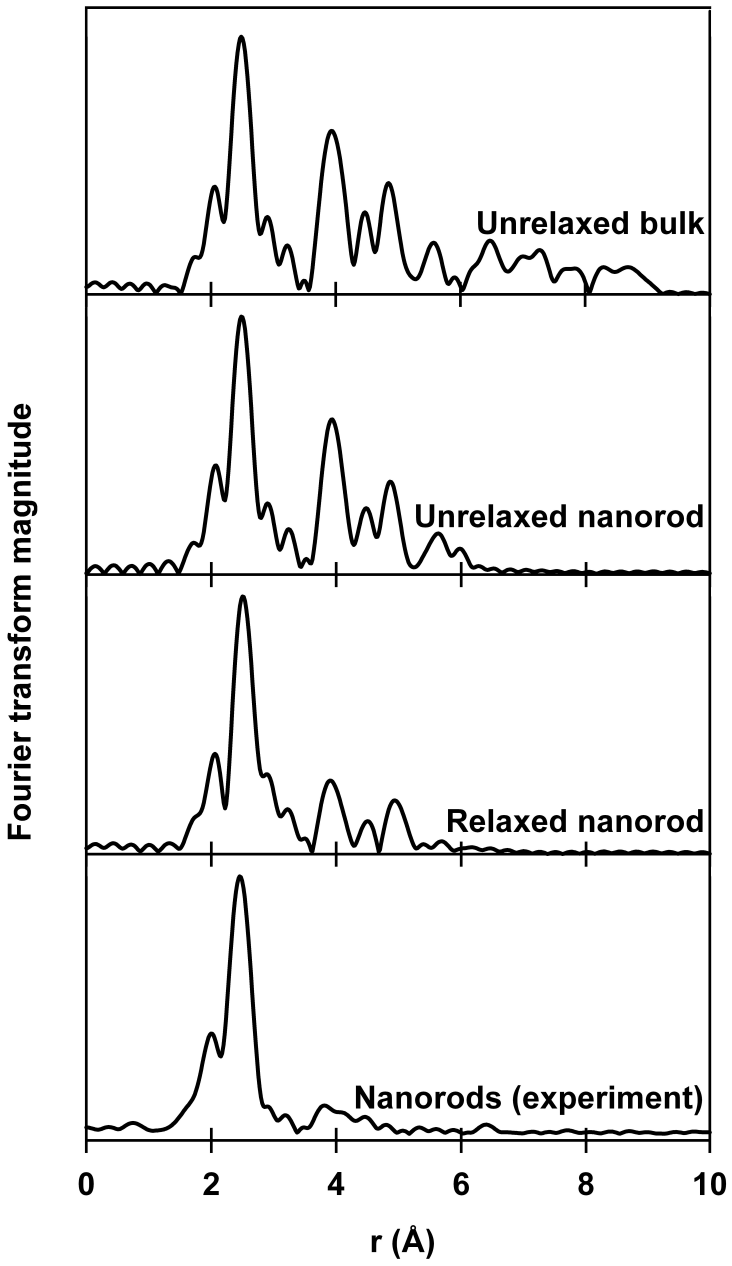

Figure S3. FEFF 8.1 was used to simulate EXAFS for calculated nanowire geometries. Pair distribution functions (PDFs) from these FEFF simulations are presented in this figure, along with an experimental PDF from the nanorods. Unrelaxed bulk and nanorod CdSe have bulk atomic positions.